ANNUAL REPORT 2008

UIUC, August 6, 2008

Modeling Heat Transfer, Precipitate Formation, and Grain Growth during Secondary Spray Cooling

Kun Xu
(PHD Student)

Department of Mechanical Science and Engineering
University of Illinois at Urbana-Champaign

Introduction: Transverse cracks

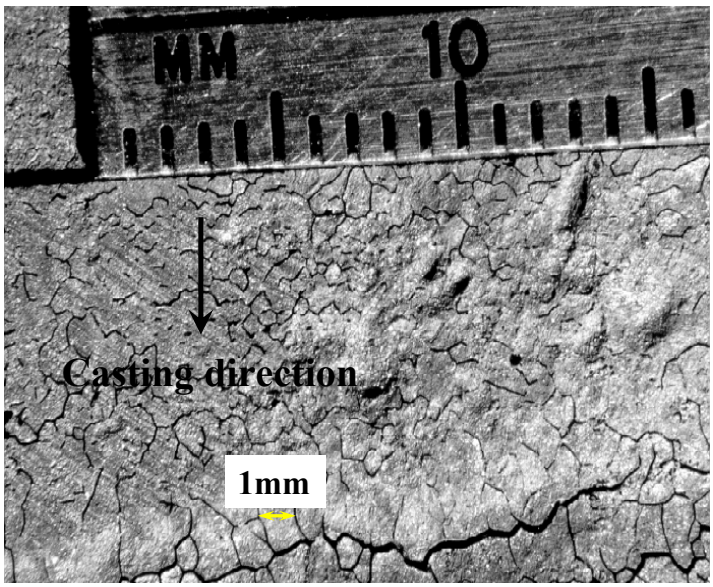

Crazing around a transverse crack at base of an oscillation mark on the as-cast top surface of a 0.2% C steel slab.

Note larger grain size at base of oscillation mark.

Typical grain size ~1mm

Reference: Reference:*E. S. Szekeres, 6th Internat. Conf. on Clean Steel, Balatonfüred, Hungary, June 2002.*

Formation of surface cracks & precipitate embrittlement

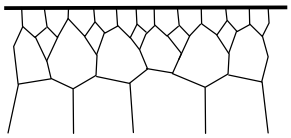

STAGE I - Normal solidification on mold wall. Surface grains are small but highly oriented.

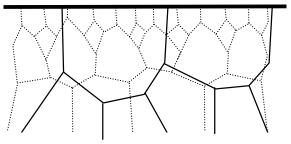

STAGE II - Surface grains "blow" locally due to high temperature (>1350°C) and strain, especially at the base of deeper oscillation marks.

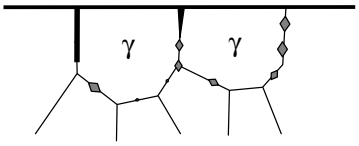

STAGE III - Nitride precipitates begin to form along the blown grain boundaries. Microcracks initiate at weak boundaries.

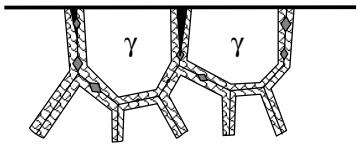

STAGE IV - Ferrite transformation begins and new precipitates form at boundaries. Existing micro-cracks grow & new ones form.

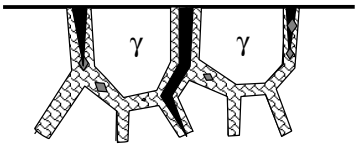

STAGE V - At the straightener, microcracks propagate and become larger cracks, primarily on top surface of the strand.

Reference: *E. S. Szekeres, 6th Internat. Conf. on Clean Steel, Balatonfüred, Hungary, June 2002.*

Effect of oscillation marks on grain size

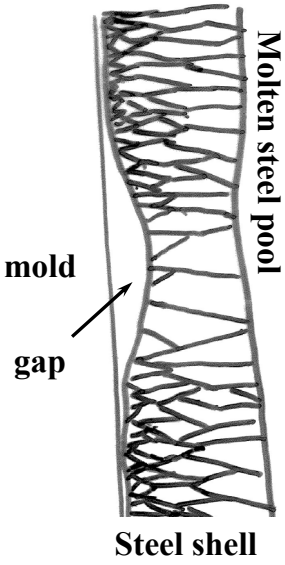

Larger grains beneath oscillation marks & surface depressions

Due to:

* more heat flow resistance across gap
* higher shell temperature
* faster grain growth rate

Causes:

* Tensile strain concentration area
* Make hot grains actually align — "secondary recrystallization"— "blown grains"
* Embrittled with a large numbers of fine precipitates at the weak grain boundaries — cracks open up along the boundaries — transverse cracks

Project Overview

- CON1D --- Temperature & Phase fraction
- Equilibrium precipitation model --- Tendency for precipitation and equilibrium concentration of all elements
- **Kinetic model for precipitate growth ---** Size distribution and volume fraction of possible precipitates
- **Grain growth model** evolving with time, cooling history with the effect of pinning precipitates --- Grain size of steel casting
- Predict ductility and transverse cracks --- Stress and strain analysis concerning coupled influence of precipitates and grain size

Final goal: Prevent cracks and assure quality

Size distribution and micrograph of AlN precipitate in CSP steel

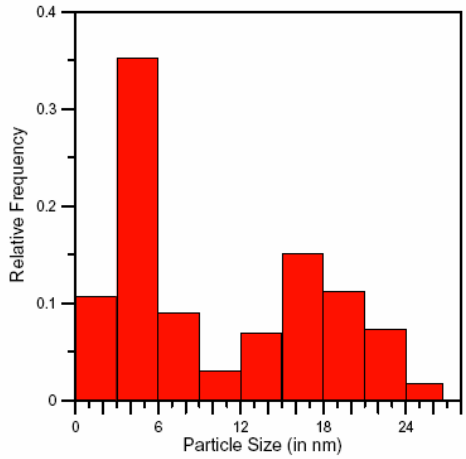

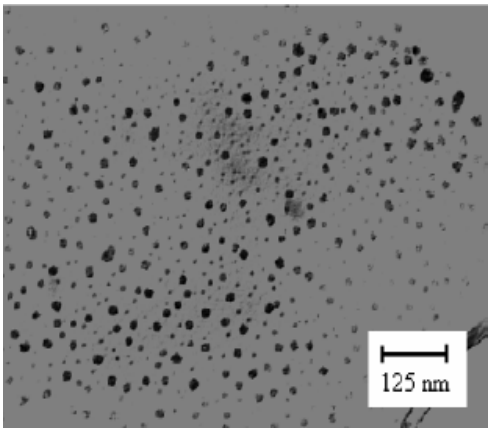

Precipitates could nucleate and grow 1) in the liquid, 2) during solidification (segregation), 3) on grain boundaries or 4) inside the grains. Composition and size distribution evolve with temperature and time.

Reference: *J. A. Garrison, Aluminum nitride precipitation behavior in thin slab material, AIST 2005 proceeding, Volume II, June 2002.*

Example Problem: multiple peak distribution

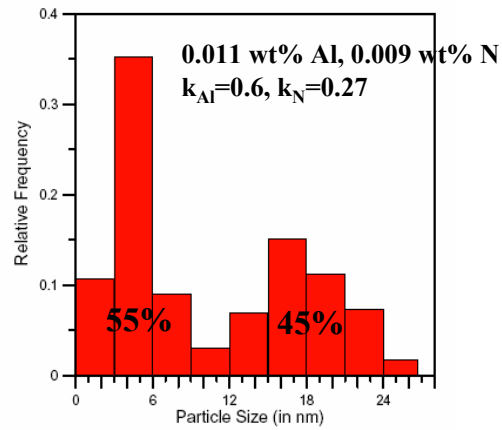

Equilibrium precipitation model calculates AlN at different stages

T_{liq}=1528.1°C, T_{sol}=1501.5°C

No AlN forming in the liquid

Differential Scheil model for segregation

AlN begins to form at 1503°C; amount formed during solidification is 6.86×10^{-4}wt%.

Equilibrium amount of AlN at 900°C is 0.01134; percent forming in solid is 94%.

Need kinetic model to correct error (94% vs 55%): Much of the AlN remaining in the solid should stay dissolved until 1060°C. At this low temperature, the nucleation and growth of new AlN particles in the solid is slow. During this time, the AlN particles already present (from solidification) can grow quickly due to local high concentration from segregation. Finally, new nuclei form in the solid at lower temperature, grow slowly from the remaining fraction of Al and N.

Introduction: Particle Collision and diffusion

Particle collision

$$\frac{dn_i}{dt} = \underbrace{-n_i \sum_{j=1}^{M}\left[(1+\delta_{ij})\Phi_{ij} n_j\right]}_{\text{Loss of particle i by collision of other particle j, double loss if both particle i}} + \underbrace{\frac{1}{2}\sum_{j=1}^{i-1}(1+\delta_{j,i-j})\Phi_{j,i-j} n_j n_{i-j}}_{\text{Generation of particle i by collision of two smaller particle j + particle i-j, only count once for two reacting particles}}$$

Particle diffusion

$$\frac{dn_i}{dt} = \underbrace{-n_i \beta_i^D n_1}_{\text{Molecule Diffusion (i→i+1)}} + \underbrace{n_{i-1}\beta_{i-1}^D n_1}_{\text{Molecule Diffusion (i-1→i)}} + \underbrace{\alpha_{i+1} A_{i+1} n_{i+1}}_{\text{Particle Dissolution (i+1→i)}} - \underbrace{\alpha_i A_i n_i}_{\text{Particle Dissolution (i→i-1)}}$$

Collision happens only in liquid, and diffusion happens both in liquid and solid

n_i : Number density of size i particle (/m^3)

Φ_{ij} : Collision coefficient for collision between size i and size j particle (m^3/s)

β_i^D : Diffusion rate constant of particle i (m^3/s)

α_i : Dissociate rate per unit area of particle i (m^{-2}s^{-1})

Particle Size Group (PSG) Model

- This model simulates nucleation (from individual molecule size 0.1nm) up to real particles (μm): particles contain from n=1 to 10^{10} molecules.
- serious computation and memory storage issues arise with so many particle sizes.
- solve problem with PSG model: use G groups of geometrically progressing size

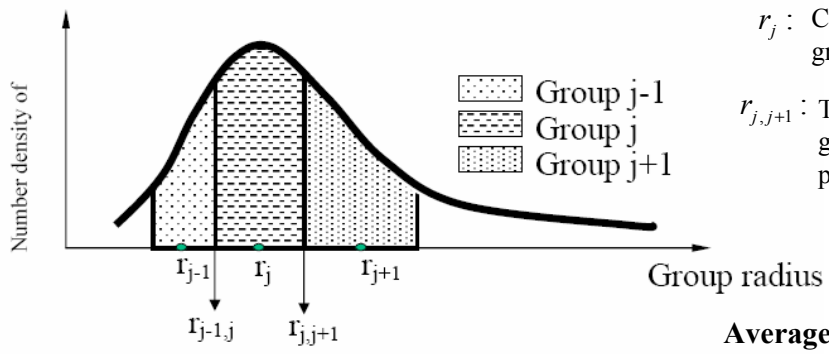

r_j : Characteristic radius of group j particle

$r_{j,j+1}$: Threshold radius between group j and group j+1 particle

$$r_{j,j+1} = \sqrt{r_j r_{j+1}}$$

Average particle volume ratio

$$R_V = \frac{V_{j+1}}{V_j} \Rightarrow r_j = R_V^{(j-1)/3} r_1$$

Total number density for each group $N_j = \int_{r_{j-1,j}}^{r_{j,j+1}} n(r)dr$

Effect of R_V on PSG collision model

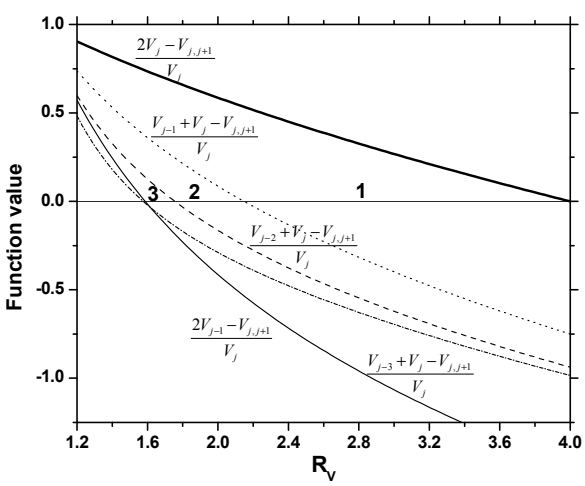

Range 1 ($4.00>R_V>2.148$)

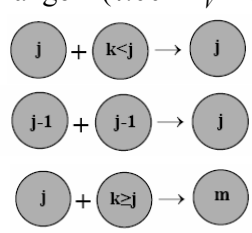

m=j+1 if k=j
m=k if k>j

Range 2 ($2.148>R_V>1.755$)

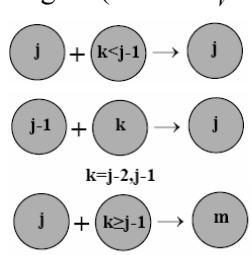

k=j-2,j-1

m=j+1 if k=j-1, j
m=j+2 if k=j+1
m=k if k>j+1

Range 3 ($1.755>R_V>1.588$)

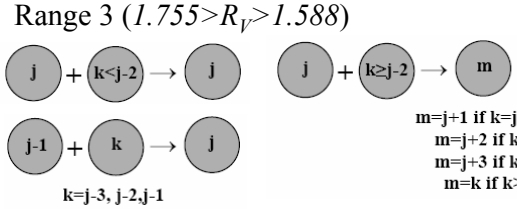

k=j-3, j-2,j-1

m=j+1 if k=j-2, j-1, j
m=j+2 if k=j+1
m=j+3 if k=j+2
m=k if k>j+2

PSG model summary for collision

$$\frac{dN_j}{dt} = \underbrace{N_j \sum_{k=1}^{k_{c,j-1}} \frac{V_k}{V_j} \Phi_{jk} N_k}_{j + k<k_{c,j} \rightarrow j} + \underbrace{\sum_{k=k_{c,j-1}}^{j-1} \frac{V_{j-1}+V_k}{V_j} \Phi_{j-1,k} N_{j-1} N_k}_{j-1 + k \rightarrow j,\ j-1 \geq k \geq k_{c,j}-1} - \underbrace{N_j \sum_{k=k_{c,j}}^{\infty} \left[(1+\delta_{jk}) \Phi_{jk} N_k \right]}_{j + k \geq k_{c,j} \rightarrow m>j}$$

$$k_{c,j} = \begin{cases} j & 4.000 > R_V > 2.148 \\ j-1 & 2.148 > R_V > 1.755 \\ j-2 & 1.755 > R_V > 1.588 \end{cases}$$

$$\frac{dN_j^*}{dt^*} = N_j^* \sum_{k=1}^{k_{c,j-1}} \frac{V_k}{V_j} (R_V^{(j-1)/3} + R_V^{(k-1)/3})^3 N_k^* + \sum_{k=k_{c,j-1}}^{j-1} \frac{V_{j-1}+V_k}{V_j} (R_V^{(j-2)/3} + R_V^{(k-1)/3})^3 N_{j-1}^* N_k^*$$
$$- N_j^* \sum_{k=k_{c,j}}^{G} (1+\delta_{jk}) (R_V^{(j-1)/3} + R_V^{(k-1)/3})^3 N_k^*$$

Generally choose $V_j = \max(R_V^{j-1}, j) V_1$ to cover the cases when $R_V < 2.0$

Validation of PSG model for collision

Total number density of particles $n_T = \sum_{i=1}^{M} n_i$ and M=1000, time step $\Delta t^* = 0.001$

Initial condition $n_1^* = 1$ and $n_i^* = 0$ for i>1 at $t^* = 0$

Boundary condition $n_M^* = 0$ at all t^*

Turbulent collision

$$\Phi_{ij} = 1.3(\varepsilon/\nu)^{1/2}(r_i + r_j)^3$$

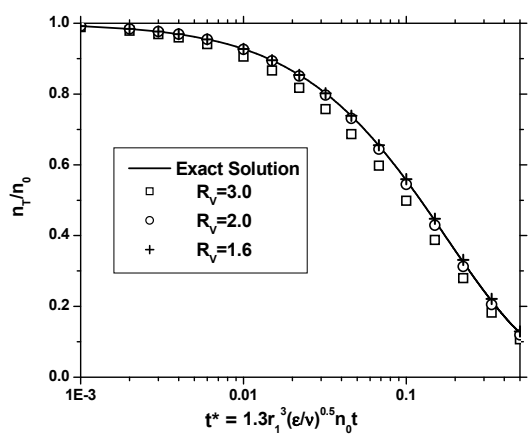

Decreasing the value of R_V can increase the accuracy of PSG model

If largest particle for exact solution has ***M*** molecules, then the number of groups ***G*** used in the PSG model must satisfy

$$R_V^{G-1} > M$$

So we choose $G = Ceil(\log_{R_V} M) + 1 + 1$

(Including boundary group $N_G \equiv 0$ at all t^*)

Validation of PSG model for collision (R_V=3.0)

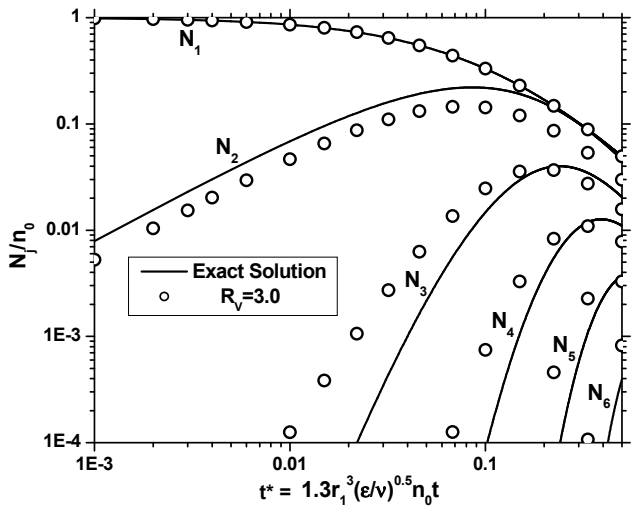

Number of groups G=8

Number range in each group

N_1: size 1
N_2: size 2-5
N_3: size 6-15
N_4: size 16-46
N_5: size 47-140
N_6: size 141-420
N_7: size 421-1262

Validation of PSG model for collision (R_V=2.0)

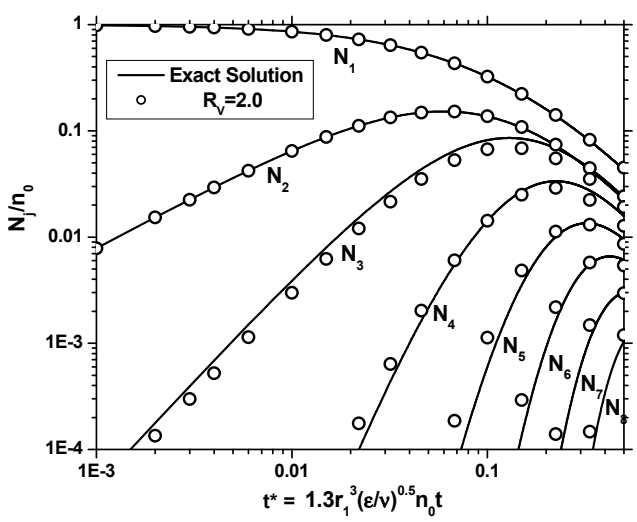

Number of groups G=12

Number range in each group

N_1: size 1
N_2: size 2
N_3: size 3-5
N_4: size 6-11
N_5: size 12-22
N_6: size 23-45
N_7: size 46-90
N_8: size 91-181
N_9: size 182-362
N_{10}:size 363-724
N_{11}:size 725-1448

Develop PSG model for diffusion

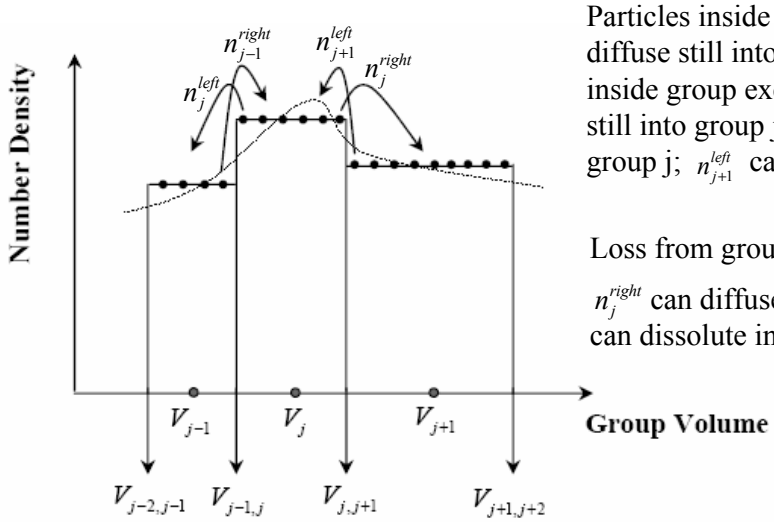

Generation to group j

Particles inside group except n_j^{right} can diffuse still into group j; particles inside group except n_j^{left} can dissolute still into group j. n_{j-1}^{right} can diffuse into group j; n_{j+1}^{left} can dissolute into group j.

Loss from group j

n_j^{right} can diffuse into group j+1; n_j^{left} can dissolute into group j-1.

PSG model for diffusion

$$\frac{dN_j}{dt} = \frac{V_1}{V_j}\beta_j^D N_1 (N_j - n_j^{right}) - \frac{V_1}{V_j}\alpha_j A_j (N_j - n_j^{left}) - \frac{Floor(V_{j,j+1})}{V_j}\beta_j^D N_1 n_j^{right}$$
$$+ \frac{Ceil(V_{j-1,j})}{V_j}\beta_{j-1}^D N_1 n_{j-1}^{right} + \frac{Floor(V_{j,j+1})}{V_j}\alpha_{j+1} A_{j+1} n_{j+1}^{left} - \frac{Ceil(V_{j-1,j})}{V_j}\alpha_j A_j n_j^{left}$$

The mass balance can be conserved by this equation. Of course, the exact distribution of particles inside each group is unknown.

$$\beta_i^D = 4\pi D r_i \qquad \alpha_i = \frac{\beta_i^D}{A_i} n_{1,eq} \exp\left(\frac{2\sigma V_m}{RTr_i}\right)$$

Define possible molecules number range inside group j particle from $V_{j-1,j}$ to $V_{j,j+1}$

$$DV_j = \max(1, Floor(V_{j,j+1}/V_1) - Ceil(V_{j-1,j}/V_1) + 1)$$

$$n_j = \frac{N_j}{DV_j} \qquad q_1 = \left(\frac{n_j}{n_{j-1}}\right)^{\frac{1}{V_j - V_{j-1}}} \qquad q_2 = \left(\frac{n_{j+1}}{n_j}\right)^{\frac{1}{V_{j+1} - V_j}}$$

$$n_j^{left} = n_{j-1} q_1^{Ceil(V_{j-1,j}) - V_{j-1}} \qquad n_j^{right} = n_j q_2^{Floor(V_{j,j+1}) - V_j}$$

Estimation of n_j^{left} and n_j^{right}

Define average number density for each group $n_j = \dfrac{N_j}{DV_j}$

And we assume

$$q_1 = \left(\frac{n_j}{n_{j-1}}\right)^{\frac{1}{V_j - V_{j-1}}}$$

$$n_j^{left} = n_{j-1} q_1^{Ceil(V_{j-1,j}) - V_{j-1}}$$

$$q_2 = \left(\frac{n_{j+1}}{n_j}\right)^{\frac{1}{V_{j+1} - V_j}}$$

$$n_j^{right} = n_j q_2^{Floor(V_{j,j+1}) - V_j}$$

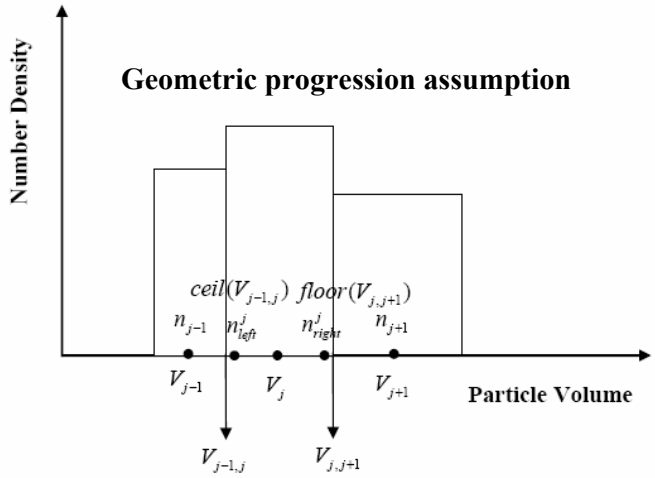

Maximum limit of n_j^{left} **and** n_j^{right} **are** N_j

Validation of PSG model for diffusion (R_V=2.0)

Define total number density of particles $n_T = \sum_{i=1}^{M} n_i$ and choose M=1000

Initial condition $n_i^* = 0$ for any size i at $t^* = 0$

Boundary condition $n_M^* = 0$ at all t^*

Total number of molecules in all size particles

$$n_S^*(t^*) = \sum_{i=1}^{M} i \cdot n_i^* = 9[1 - \exp(-0.1t^*)]$$

Choose time step $\Delta t^* = 0.01$

Supersaturation $\Pi = \dfrac{n_1}{n_{1,eq}} = n_1^* \Rightarrow \Pi_{\max} \approx 4$

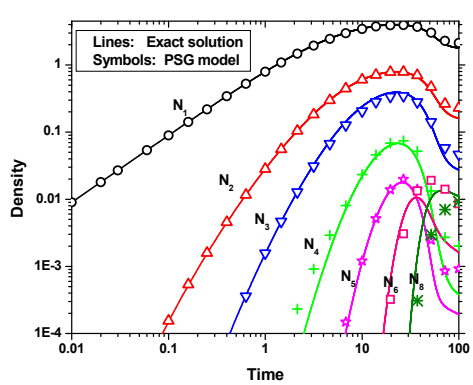

Good match for just *G=12* groups

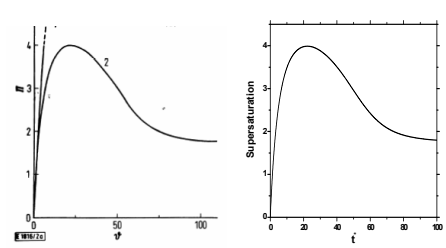

L. Kampmann and M. Kahlweit, "On the Theory of Precipitations II," Berichte der Bunsen-Gesellschaft physikalische Chemie, Vol. 74 (5), 1970, 456-462.

Further PSG model validation: Extend test problem to physical size distribution

$$V_m = 6.4\times10^{-5} m^3/mol,\ r_1 = 0.294nm,\ T = 300K,\ D = 10^{-9} m^2/s$$

$$\sigma = 0.02J/m^2,\ N_{1,eq} = 6\times10^{23} m^{-3},\ r_i = r_1 i^{1/3},\ t^* = 2.216\times10^6 t$$

$$\Pi_{\max} \approx 4 \Rightarrow r_c = \frac{2\sigma V_m}{RT\ln\Pi_{\max}} \approx 0.742nm \Rightarrow i_c \approx 16 \Rightarrow N_5$$

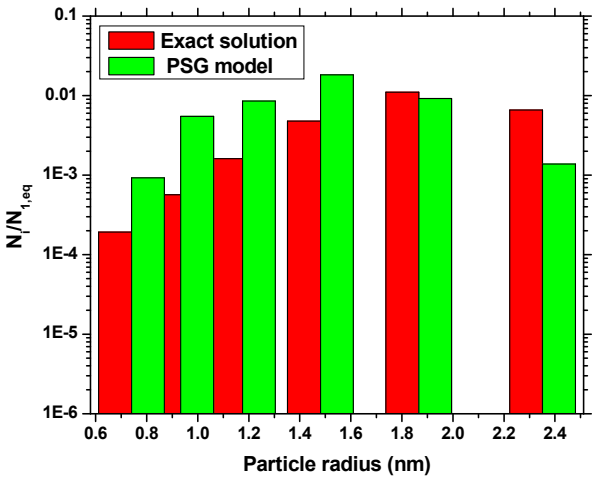

t=45.1μs

N_5: size 12-22 (0.673-0.824nm)
N_6: size 23-45 (0.836-1.045nm)
N_7: size 46-90 (1.053-1.317nm)
N_8: size 91-181 (1.322-1.662nm)
N_9: size 182-362 (1.665-2.094nm)
N_{10}:size 363-724 (2.096-2.639nm)

AlN Calculation in Compact Strip Production

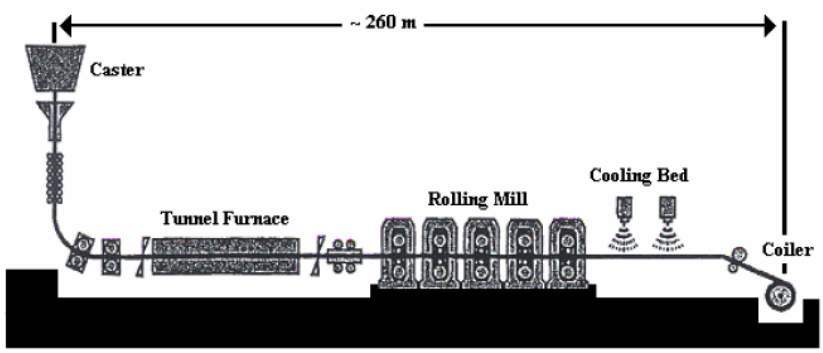

Figure 1. Schematic of CSP process[5].

$$V_m = 1.33\times10^{-5} m^3/mol,\ r_1 = 0.174nm,\ \sigma = 0.75J/m^2$$

Chemical composition: 0.06wt% C, 0.462% Mn, 0.004% P, 0.004% S, 0.017% Si, 0.011% Al, 0.009% N

Solubility of AlN in austenite

Solubility product: $\log K_{AlN} = -\frac{6770}{T} + 1.03$

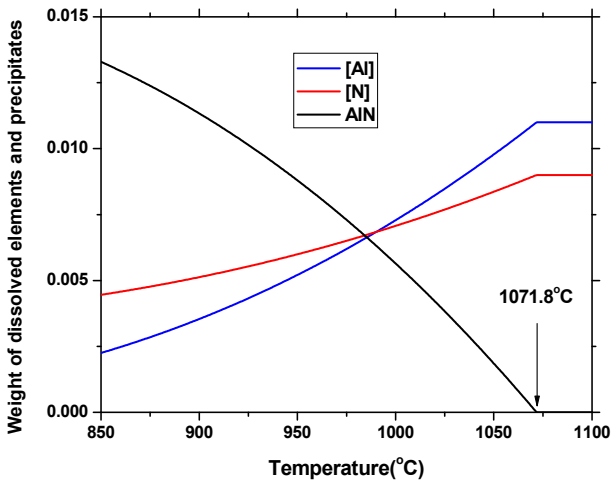

$$[Al][N] = K_{AlN}$$

$$\frac{Al_0 - [Al]}{M_{Al}} = \frac{N_0 - [N]}{M_N}$$

Focus calculation from 1071.8°C to 900°C

Diffusion of Al and N in austenite

Diffusion coefficient: $D_{Al} = 3\times10^{-3}\exp\left(-\frac{234500}{RT}\right)$

$$D_N = 9.1\times10^{-5}\exp\left(-\frac{168500}{RT}\right)$$

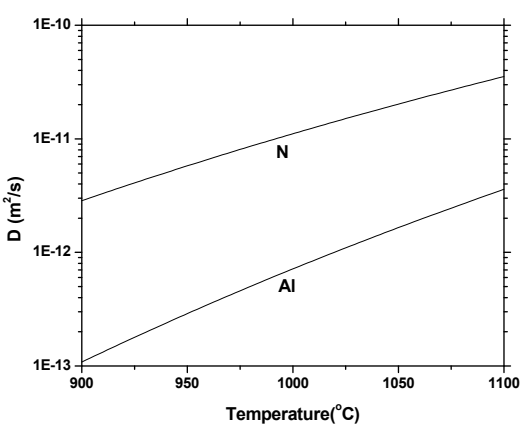

Choose diffusion of Al (for β_j^D and α_j) to calculate the formation of AlN (since Al diffuses much slower than N and mole fraction of N is larger than that of Al)

Calculation of AlN size distribution

$$\rho_{steel} = 7.8\times10^3 kg/m^3 \qquad N_M = \frac{Al_0 \times \rho_{steel}}{M_{Al}} N_A \approx 1.9144\text{e+025/m}^3$$

$$N_s = N_M\left[1.0 - \exp(-0.001 * 4\pi D r_1^* * N_M * t)\right]$$

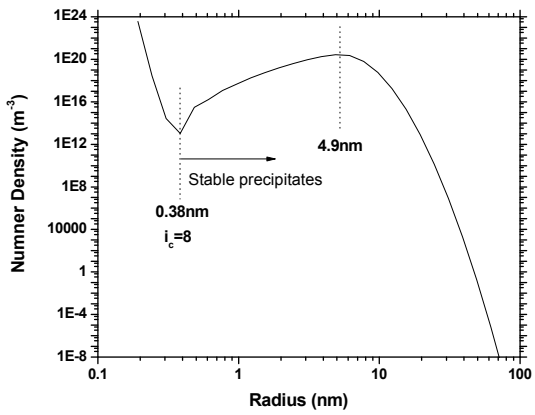

Typical cooling rate $\Delta T / \Delta t \approx 20^o C / s$

$\Rightarrow$ *Total time* $t \approx 8.6s$

G=40, packing factor 0.74
Radius 0.174nm~1.58μm
1~5.5×10^{11} molecules

Current time step $\Delta t = 4*10^{-8}s$ for stability, implicit format needs to be considered in the future work if the processing time is larger

Compare AlN size distribution with measurement

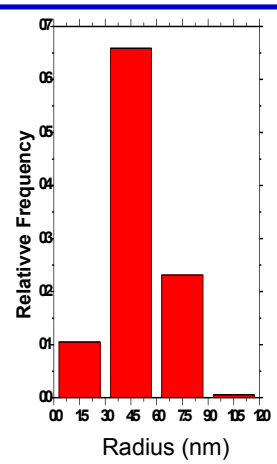

Simulation

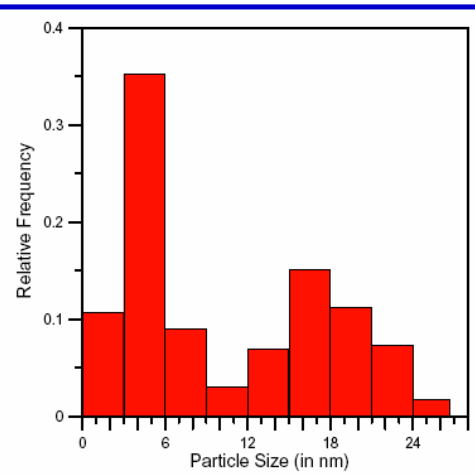

Experiment

Good match with small-size precipitate distribution (governed by solid-state diffusion).

Need to include liquid collisions, solidification segregation and subsequent growth to model larger AlN particles.

The influence of pinning precipitates on the grain growth

➢ Grain growth model in the presence of growing precipitates

$$\frac{d\bar{D}}{dt} = M_0^* \exp\left(-\frac{Q_{app}}{RT}\right)\left[\frac{1}{\bar{D}} - \frac{1}{k}\frac{f}{r}\right]^{(1/n-1)}$$

Update the f/r value for the growing precipitates for each step

Some parameters to fit grain size for mainly Ti-microalloyed or Nb-microalloyed steels are given, but the influence of combined effect of many alloying elements still needs more work

$$I_1 = M_0^* \int_{t1}^{t2} \exp\left(-\frac{Q_{app}}{RT}\right)dt \qquad \bar{D}_{Lim}^0 = k\frac{r_0}{f_0}$$

$$I_2 = c_1 \int_{t1}^{t2} \frac{1}{T}\exp\left(-\frac{Q_s}{RT}\right)dt \qquad m = \left(\frac{k}{f_0}\right)\frac{I_2}{I_1}$$

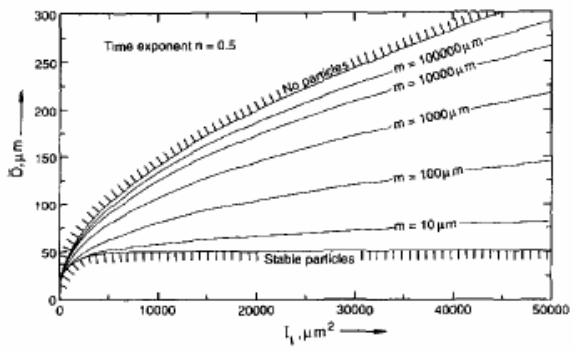

Fig. 7. Predicted variation in average grain size ($\bar{D}$) with I_1 and m for $\bar{D}_{Lim}^0 = 50\ \mu m$, $n = 0.5$, and $\bar{D}_0 = 0$ (growing precipitates).

Constant volume fraction $\mathbf{f_0}$ for precipitate

Reference: I. Anderson, O. Grong, Acta Metall. mater. Vol. 43, No. 7, pp2673-2688, 1995.

Kinetic model for austenite grain growth

➢ Grain growth model

$$\frac{d\bar{D}}{dt} = M_0^* \exp\left(-\frac{Q_{app}}{RT}\right)\left[\frac{1}{\bar{D}} - \frac{1}{k}\frac{f}{r}\right]^{(1/n-1)}$$

When temperature drops into mixed-phase region (transformation at ~800°C), then the ferrite will form and brand new grains cause the cracks much more difficult to form. And the already existing grains in austenite almost will not change because of low growth rate at low temperature

CW: secondary cooling intensity

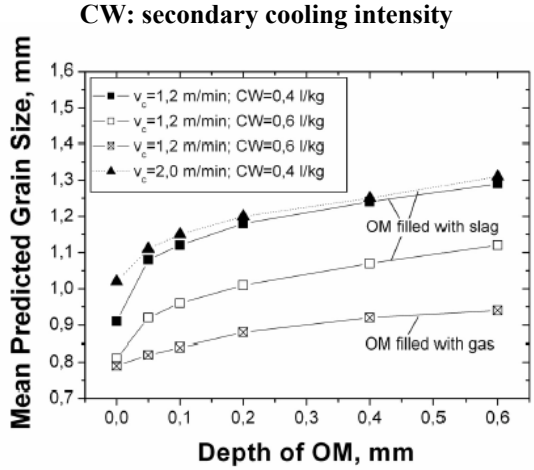

The change of depth of oscillation marks influences the temperature history at these locations. Larger depth causes higher temperature and thus larger grain size beneath oscillation marks.

Reference: C. Bernhard, J. Reiter, Simulation of austenite grain growth in continuous casting, AISTech 2007.

Validation of austenite grain size model

$$M_0^* = 4\times10^{-3} m^2/s,\ n = 0.5 \qquad Q_{app} = 167686 + 40562(wt\%C_P)$$

$$wt\%C_P = wt\%C - 0.14wt\%Si + 0.04wt\%Mn$$

Calculation from starting temperature given to 900°C

The average cooling rate 5°C/s

initial grain size is zero

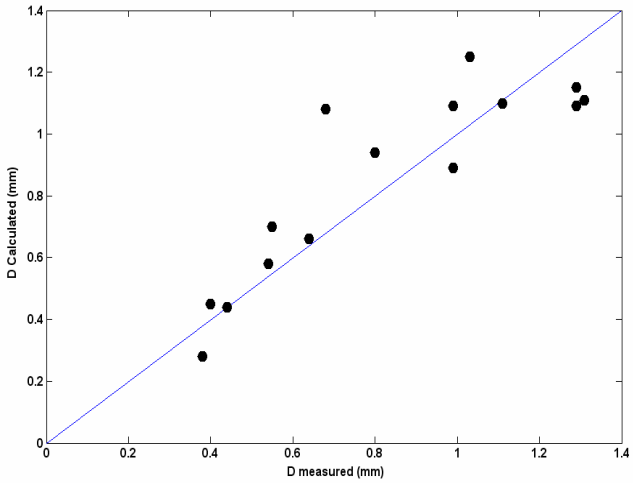

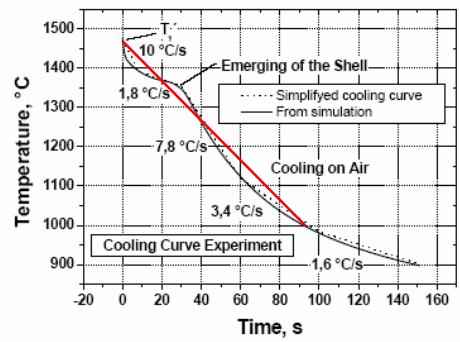

Reference: J. Reiter, C. Bernhard, H Presslinger, Determination and prediction of austenite grain size in relation to product quality of the continuous casting process, MS&T 06, Cincinnati, USA.

Grain growth in real continuous casting

Name	%C	%Mn	%Si	%Ti	%Nb	%V	%B	%N
1006	0.06	1	0.2	0.015	0.015	0.004	0.006	0.01

Mold length: 0.95m
Start of first spray zone: 0.85m
End of last spray zone: 11.25m

T_{liq}=1524.0°C, T_{sol}=1498.5°C
Calculation is from liquidus temperature and initial grain size is zero

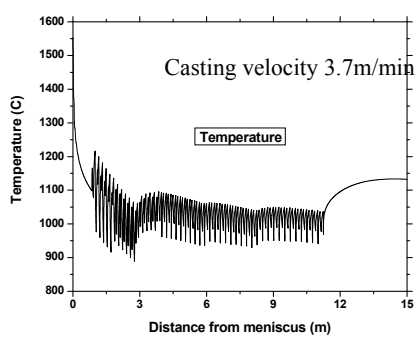

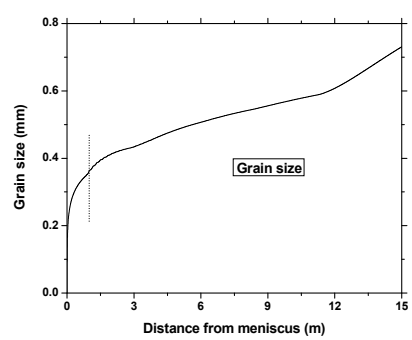

Grain size at solidus temperature ~0.159mm

By cooling rate from T_{liq} to T_{sol} C_R=105.4°C/s

$\lambda_1 = K(C_R)^m(C_0)^n$ ~0.184mm

Conclusions for precipitates

1) The precipitates can form in the different stages. This causes different locations (removed from liquid, between dendrites, on the grain boundary or inside the grain) and different number and size distributions of precipitates. Our equilibrium precipitation model can predict tendency of precipitation for different stages and explain multiple peak size distribution qualitatively
2) The PGS model gives a good match for particle collision within a wide range of R_V and accuracy increases with decreasing values of R_V
3) A new PSG method is developed for particle diffusion. The results match the exact Kampmann case with reasonable error. This model makes it possible to simulate precipitates distribution for realistic processes with tolerable computation resources

Conclusions for grain growth

4) The results from austenite grain growth model can match the experimental grain size for a wide range of chemical composition
5) Grain growth model is applied to simulate a practical continuous casting process. Starting from a reasonable small initial size, the grains approach 60% of their final grain size by mold exit. Without precipitates, they are large enough to cause ductility problems.
6) The higher temperature and the corresponding larger grain growth rate and lack of fine precipitates are likely the controlling factors to cause coarse grains and susceptibility to cracks especially beneath oscillation mark roots

Future work

1) Consider local different concentrations of element due to segregation into the kinetic PSG model to analyze the volume fraction and size distribution of the precipitates forming at different stages
2) The kinetic PSG model needs to extend to complex system with possible multi precipitates formation and simulate precipitates evolution for the practical steel grades
3) With the knowledge of the steel chemical compositions and cooling history, coupled precipitate and grain growth model can be used to predict and track precipitate formation and the grain size in a more physical and accurate way, especially larger grains beneath oscillation marks from different temperature history
4) Consider the relation between the tensile stress (or strain) and grain size at the presence of precipitates on the intergranular fracture (finally prevent cracks and assure quality)

Acknowledgements

- Continuous Casting Consortium Members (Baosteel, Corus, Goodrich, Labein, LWB Refractories, Mittal, Nucor, Postech, Steel Dynamics, Ansys Inc.)
- Prof B.G.Thomas
- Other Graduate students of CCC group

Thank you for attendance!